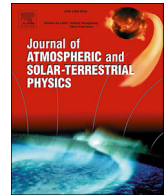




Contents lists available at ScienceDirect

Journal of Atmospheric and Solar-Terrestrial Physics

journal homepage: www.elsevier.com/locate/jastp

Predicting solar surface large-scale magnetic field of Cycle 24

Jie Jiang^{a,b,*}, Jinbin Cao^a^a School of Space and Environment, Beihang University, Beijing, China^b Key Laboratory of Solar Activity, National Astronomical Observatories, Chinese Academy of Sciences, Beijing, 100012, China

ARTICLE INFO

Keywords:

Solar activity
Prediction
Solar magnetic fields
Solar polar fields

ABSTRACT

The Sun's surface field, especially the polar field, sets the boundary condition for the coronal and heliospheric magnetic fields, but also provides us insight into the dynamo process. The evolution of the polar fields results from the emergence and subsequent evolution of magnetic flux through the solar surface. In this paper we use a Monte Carlo approach to investigate the evolution of the fields during the decay phase of cycle 24. Our simulations include the emergence of flux through the solar surface with statistical properties derived from previous cycles. The well-calibrated surface flux transport model is used to follow the evolution of the large-scale field. We find the polar field can be well reproduced one year in advance using the observed synoptic magnetograms as the initial condition. The temporary variation of the polar field measured by Wilcox Solar Observatory (WSO), e.g., the strong decrease of the south polar field during 2016–2017 which is not shown by SDO/HMI and NSO/SOLIS data usually is not well reproduced. We suggest observational effects, such as the effect of the large gradient of the magnetic field around the southern polar cap and the low resolution of WSO might be responsible. The northern hemisphere polar field is predicted to increase during 2017. The southern polar field is predicted to be stable during 2017–2018. At the end of 2017, the magnetic field in two poles is predicted to be similar (although of opposite polarities). The expected value for the dipole moment around 2020 is 1.76 ± 0.68 G and 2.11 ± 0.69 G based on the initial conditions from SDO/HMI and NSO/SOLIS synoptic magnetograms, respectively. It is comparable to that observed one at the end of Cycle 23 (about 1.6G based on SOHO/MDI).

1. Introduction

Prediction of short-term and long-term future levels of solar activity has found much interest in the literature since solar activity is the driver of space weather, which has practical consequences for human activities in space. A reliable method of long-term prediction could also provide constraints on dynamo models.

Sunspots are the most direct demonstration of solar activity. Most long-term predictions of solar activity concentrate on the prediction of the time evolution of the sunspot number (Hathaway et al., 1994; Li et al., 2005; Gholipour et al., 2005; Hiremath, 2008; Podladchikova and van der Linden, 2012) based on the extrapolation method or the precursor methods, see Petrovay (2010) for more details. Among the most reliable techniques are those that use geomagnetic activity at or near the time of minimum as the precursors for future cycle amplitude (Schatten et al., 1978; Schatten, 2005). Geomagnetic activity during the preceding cycle at or near the time of minimum corresponds to the axial dipole field (Wang and Sheeley, 2009). The good predictive abilities of the geomagnetic indexes support the Babcock-Leighton (BL) type of solar

dynamo, in which surface poloidal field is the source of the next cycle strength. Since the source of the cycle strength in the BL dynamo is observable, it makes the dynamo-based solar cycle prediction feasible. The dynamo-based predictions started around the end of cycle 23 by two groups (Dikpati and Gilman, 2006; Choudhuri et al., 2007; Jiang et al., 2007), who gave opposite predictions of Cycle 24 strength. See Section 4 of Karak et al. (2014) for the differences of two models. Although the dynamo-based predictions attempted to model the time evolution of the magnetic field below and over the solar surface, they cannot predict the details of the features of solar cycle, i.e. shapes of the solar cycle and the time evolution of the polar field.

Apart from their role in the solar dynamo, the polar field are of great importance in determining the global structure of the corona, e.g. (Hayashi et al., 2008; Hayashi, 2013), the heliospheric magnetic fields, the propagation of galactic cosmic rays throughout the heliosphere and so on. However, owing to foreshortening effects at the solar limb, it is hard to accurately measure the evolution of the polar fields. Determinations of the polar fields are further complicated by the variable B_0 angle of the Sun's rotation axis with respect to the ecliptic (Petrie, 2015;

* Corresponding author. School of Space and Environment, Beihang University, Beijing, China.
E-mail address: jiejiang@buaa.edu.cn (J. Jiang).

<http://dx.doi.org/10.1016/j.jastp.2017.06.019>

Received 15 March 2017; Received in revised form 7 June 2017; Accepted 29 June 2017

Available online xxx

1364-6826/© 2017 Elsevier Ltd. All rights reserved.

Wang, 2016).

Magnetic flux generated by the dynamo process in the interior emerges at the solar surface in the form of bipolar magnetic regions (BMRs) with a preferred tilt of the axis joining the two polarities with respect to the equator. The emerged flux is then transported and dispersed over the solar surface due to systematic and turbulent motions. When magnetic flux elements of opposite polarity comes into contact, the features cancel, removing equal amounts of flux of each sign. Because of the systematic tendency of the tilt angle, a net flux is transported across the equator during each cycle. This leaves a net surplus of following flux in each hemisphere which is carried poleward by the surface meridional flow. The accumulation of these remnants of BMRs eventually neutralizes, reverses, and builds up the polar field for the next cycle as the sunspot cycle progresses. The whole process can be well simulated by the Surface Flux Transport (SFT) models (Wang et al., 1989; van Ballegooyen et al., 1998; Baumann et al., 2004; Yeates et al., 2007). The model show remarkable success in reproducing the evolution of the Sun's large-scale field over surface, although some differences including the transport parameters and the methods to treat the flux source term, are used by different authors.

The success of the SFT model in reproducing the large-scale field demonstrates its functionality and potential for predicting the large-scale field evolution (Schrijver and De Rosa, 2003). Based on the statistical properties of solar cycle, we may predict the sunspot emergence. With the help of the SFT model, people can get the possible large-scale field evolution over the surface, including the polar field and the axial dipole moment a few years in advance. In this study, we aim to predict the sunspot emergence, polar field strengths, the appearance of the magnetic butterfly diagram during 2017–2020, and the strength of cycle 25. The differences from Cameron et al. (2016) concentrate on three aspects. Firstly, we have slightly improved the empirically derived statistics of the solar cycle variation of the sunspot group emergence. Secondly, we include predictions for the polar field strength and the magnetic butterfly for the rest of cycle 24. Thirdly, we updated the prediction of cycle 25 based on the assimilation of the most recent data into the model.

The paper is organized as follows. In Section 2, we present our improved description of sunspot emergence properties based on the solar cycle properties. The details about the SFT model are given in Section 3. In Section 4, we give our predicted results about the large-scale field evolution during 2017–2020 and the possible strength of cycle 25.

2. Prediction of sunspot emergence

A main ingredient of the SFT model is the emergence of bipolar magnetic fields. In this section we present an improved description of the sunspot group emergence, which includes the number, location, area, and tilt angle, and the empirical statistical properties were used to derive them.

Comparing with Cameron et al. (2016), we made the following improvement in deriving the time evolution of the BMR emergence. Firstly, the new version of the monthly sunspot number (R) (Clette et al., 2014)¹ was used here. Based on the sunspot data since 1878 onwards, the number of BMRs emerging per month was taken to be equal to $R_G = 0.24R$. The functional form of R_G is $R_G = f(t) + \Delta f(t)$, where $f(t)$ was given by Equation (1) of Hathaway et al. (1994). It is $f(t) = a(t - t_0)^3 / \{ \exp[(t - t_0)^2 / b^2] - c \}$, where $b(a) = 27.12 + 25.15/(a \times 10^3)^{1/4}$ and $c = 0.71$. The values for parameters a (amplitude) and t_0 (starting time) to get $f(t)$ are 0.0018 and 2008.98. $\Delta f(t)$ denotes the random scatter of the time evolution of the sunspot number. The left panel of Fig. 1 shows the evolution of the ratio (r) between $\Delta f(t)$ and $f(t)$ for cycles 21–23. The right panel shows the evolution of the standard deviation of the ratio (σ_r) with one year bin size for the three

different cycles. The symbol of black triangle is the averaged values. The fitted function of the standard deviation of the ratio excluding the first two year when there is large scatters due to the cycle overlap is $\sigma_r = 0.55 - 0.16t - 0.016t^2$.

The latitudinal distribution and the mean tilt angle were studied by Jiang et al. (2011). Since the new sunspot record was used here, we recalculated the relation between the mean latitudes λ_n and cycle strength S_n for different cycle n using the method suggested by Jiang et al. (2011). The latitudinal distribution is $\lambda_n = 12.2 + 0.015S_n$. For the scatter of latitude distribution (standard deviation σ_n^i for cycle n at i th phase of the cycle), we excluded points deviating from the mean by more than $2\sigma_n^i$ in Jiang et al. (2011); Cameron et al. (2016), which caused the sharp boundary of the butterfly diagram compared with the observations. Here we only exclude points deviating from the mean by more than $2.2\sigma_n^i$ on the equatorward side in order to better reproduce the butterfly diagram. The mean tilt angle, α_n , obeys $\alpha_n = T_n \sqrt{|\lambda|}$. The relation between T_n and S_n is taken as $T_n = 1.72 - 0.0022S_n$. For the scatter of the tilt angle, we used the empirical relation which depends on sunspot umbral area, i.e., Equation (1) of Jiang et al. (2014). The resulting tilt angle is multiplied by a factor 0.7 to include the effect of inflow towards the activity belts (Cameron and Schüssler, 2010; Jiang et al., 2010; Martin-Belda and Cameron, 2016, 2017). The area distribution is based on the Equations 12–14 of Jiang et al. (2011). The BMRs have a random distribution in longitudes.

We made a Monte Carlo analysis using 50 realizations of sunspot emergence generated from the standard deviation of time evolution of sunspot group number. Fig. 2 shows the comparison of the actual monthly sunspot number (left panel) and of the butterfly diagram (right panel) with the random realizations based on the statistical relations. The blue shading indicates the $\pm 2\sigma$ variation of 50 random realizations. The observed monthly sunspot number are almost within the shading. The red curve is an example for one realization of random source of Cycle 24.

Comparing to Fig. 1 of Cameron et al. (2016), Fig. 2 is closer to the observational case. There is a larger scatter for the sunspot number during the decay phase, which plays important roles in the polar field strength at the end of the cycle since they have low latitude distribution (Cameron et al., 2013; Jiang et al., 2014). The butterfly diagram is more similar to the observed one, especially near the boundaries of the butterfly wings.

3. Surface flux transport modelling

3.1. Surface flux transport model

With the sunspot group emergences as the source of the surface magnetic flux, the SFT model can be used to study the evolution of the magnetic field over the surface. The model treats the evolution of the radial component of the large-scale magnetic field B at the solar surface resulting from passive transport by convection (treated as a diffusivity), differential rotation Ω , and meridional flow v . The corresponding equation is

$$\frac{\partial B}{\partial t} = -\Omega(\theta) \frac{\partial B}{\partial \phi} - \frac{1}{R_\odot \sin \theta} \frac{\partial}{\partial \theta} [v(\theta)B \sin \theta] + \frac{\eta}{R_\odot^2} \left[\frac{1}{\sin \theta} \frac{\partial}{\partial \theta} \left(\sin \theta \frac{\partial B}{\partial \theta} \right) + \frac{1}{\sin^2 \theta} \frac{\partial^2 B}{\partial \phi^2} \right] + S(\theta, \phi, t), \quad (1)$$

where θ and ϕ are heliographic colatitude and longitude, respectively. The magnetic diffusivity, η describes the random walk of the magnetic flux elements as transported by supergranulation flows. The source term, $S(\theta, \phi, t)$, describes the emergence of magnetic flux at the solar surface. The time evolution of S is obtained using the randomly realized sunspot emergence in Section 2.

We take the same flux transport parameters, i.e., $\Omega(\theta)$, $v(\theta)$ and η as

¹ <http://www.sidc.be/silso/datafiles>.

Download English Version:

<https://daneshyari.com/en/article/8139140>

Download Persian Version:

<https://daneshyari.com/article/8139140>

[Daneshyari.com](https://daneshyari.com)